Bohr!helium
Rutherford
helium
three body@3-body problem

Chapter 41

Helium atom

preceed this by a chapter on 3-disk quantum scattering

> "But," Bohr protested, "nobody will believe me unless I can explain every atom and every molecule." Rutherford was quick to reply, "Bohr, you explain hydrogen and you explain helium and everybody will believe the rest."
> John Archibald Wheeler (1986)

(G. Tanner)

So far much has been said about 1-dimensional maps, game of pinball and other curious but rather idealized dynamical systems. If you have become impatient and started wondering what good are the methods learned so far in solving real physical problems, we have good news for you. We will show in this chapter that the concepts of symbolic dynamics, unstable periodic orbits, and cycle expansions are essential tools to understand and calculate classical and quantum mechanical properties of nothing less than the helium, a dreaded three-body Coulomb problem.

This sounds almost like one step too much at a time; we all know how rich and complicated the dynamics of the three-body problem is – can we really jump from three static disks directly to three charged particles moving under the influence of their mutually attracting or repelling forces? It turns out, we can, but we have to do it with care. The full problem is indeed not accessible in all its detail, but we are able to analyze a somewhat simpler subsystem – collinear helium. This system plays an important role in the classical dynamics of the full three-body problem and its quantum spectrum.

The main work in reducing the quantum mechanics of helium to a semiclassical treatment of collinear helium lies in understanding why we are allowed to do so. We will not worry about this too much in the beginning; after all, 80 years and many failed attempts separate Heisenberg, Bohr and others in the 1920ties from the insights we have today on the role chaos plays for helium and its quantum spectrum. We have introduced collinear helium and learned how to integrate its trajectories in sect. 7.3.

action!helium
Kustaanheimo-Stiefel transformation

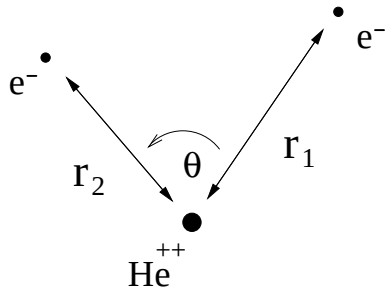

Figure 41.1: Coordinates for the helium three body problem in the plane.

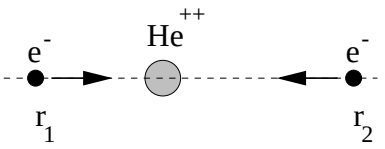

Figure 41.2: Collinear helium, with the two electrons on opposite sides of the nucleus.

Here we will find periodic orbits and determine the relevant eigenvalues of the fundamental matrix in sect. 41.1. We will explain in sect. 41.5 why a quantization of the collinear dynamics in helium will enable us to find parts of the full helium spectrum; we then set up the semiclassical spectral determinant and evaluate its cycle expansion. A full quantum justification of this treatment of helium is briefly discussed in sect. 41.5.1.

41.1 Classical dynamics of collinear helium

Recapitulating briefly what we learned in sect. 7.3: the collinear helium system consists of two electrons of mass m_e and charge $-e$ moving on a line with respect to a fixed positively charged nucleus of charge $+2e$, as in figure 41.2.

The Hamiltonian can be brought to a non–dimensionalized form

$$H = \frac{p_1^2}{2} + \frac{p_2^2}{2} - \frac{2}{r_1} - \frac{2}{r_2} + \frac{1}{r_1 + r_2} = -1\,. \tag{41.1}$$

The case of negative energies chosen here is the most interesting one for us. It exhibits chaos, unstable periodic orbits and is responsible for the bound states and resonances of the quantum problem treated in sect. 41.5.

There is another classical quantity important for a semiclassical treatment of quantum mechanics, and which will also feature prominently in the discussion in the next section; this is the classical action (34.15) which scales with energy as

$$S(E) = \oint \mathrm{d}\mathbf{q}(E)\cdot\mathbf{p}(E) = \frac{e^2 m_e^{1/2}}{(-E)^{1/2}}\, S, \tag{41.2}$$

with S being the action obtained from (41.1) for $E = -1$, and coordinates $\mathbf{q} = (r_1, r_2)$, $\mathbf{p} = (p_1, p_2)$. For the Hamiltonian (41.1), the period of a cycle and its action are related by (34.17), $T_p = \frac{1}{2} S_p$.

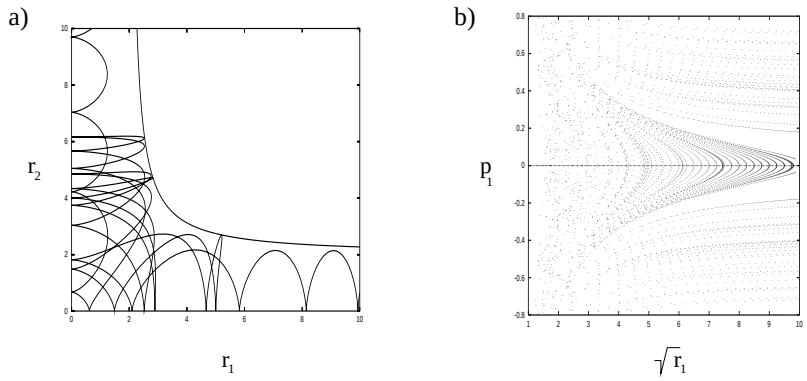

Figure 41.3: (a) A typical trajectory in the $r_1 - r_2$ plane; the trajectory enters here along the r_1 axis and escapes to infinity along the r_2 axis; (b) Poincaré map (r_2=0) for collinear helium. Strong chaos prevails for small r_1 near the nucleus.

After a Kustaanheimo–Stiefel transformation

$$r_1 = Q_1^2\,, \qquad r_2 = Q_2^2\,, \qquad p_1 = \frac{P_1}{2Q_1}\,, \qquad p_2 = \frac{P_2}{2Q_2}\,, \tag{41.3}$$

and reparametrization of time by $d\tau = dt/r_1 r_2$, the equations of motion take form (7.18)

41.1 page 794

$$\begin{aligned} \dot{P}_1 &= 2Q_1\left[2 - \frac{P_2^2}{8} - Q_2^2\left(1 + \frac{Q_2^2}{R_{12}^4}\right)\right]; \qquad \dot{Q}_1 = \frac{1}{4}P_1 Q_2^2 \\ \dot{P}_2 &= 2Q_2\left[2 - \frac{P_1^2}{8} - Q_1^2\left(1 + \frac{Q_1^2}{R_{12}^4}\right)\right]; \qquad \dot{Q}_2 = \frac{1}{4}P_2 Q_1^2. \end{aligned} \tag{41.4}$$

Individual electron–nucleus collisions at $r_1 = Q_1^2 = 0$ or $r_2 = Q_2^2 = 0$ no longer pose a problem to a numerical integration routine. The equations (7.18) are singular only at the triple collision $R_{12} = 0$, i.e., when both electrons hit the nucleus at the same time.

The new coordinates and the Hamiltonian (7.17) are very useful when calculating trajectories for collinear helium; they are, however, less intuitive as a visualization of the three-body dynamics. We will therefore refer to the old coordinates r_1, r_2 when discussing the dynamics and the periodic orbits.

41.2 Chaos, symbolic dynamics and periodic orbits

Let us have a closer look at the dynamics in collinear helium. The electrons are attracted by the nucleus. During an electron–nucleus collision momentum is transferred between the inner and outer electron. The inner electron has a maximal screening effect on the charge of the nucleus, diminishing the attractive force on the outer electron. This electron – electron interaction

fundamental!domain!collinear helium
helium!collinear!fundamental domain

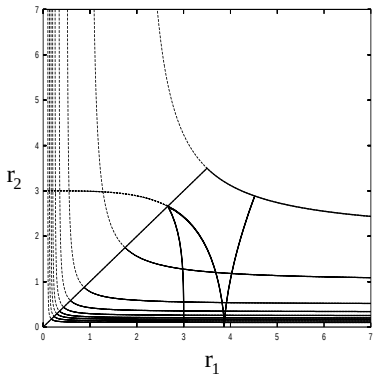

Figure 41.4: The cycle 011 in the fundamental domain $r_1 \geq r_2$ (full line) and in the full domain (dashed line).

is negligible if the outer electron is far from the nucleus at a collision and the overall dynamics is regular like in the 1-dimensional Kepler problem.

Things change drastically if both electrons approach the nucleus nearly simultaneously. The momentum transfer between the electrons depends now sensitively on how the particles approach the origin. Intuitively, these nearly missed triple collisions render the dynamics chaotic. A typical trajectory is plotted in figure 41.3 (a) where we used r_1 and r_2 as the relevant axis. The dynamics can also be visualized in a Poincaré surface of section, see figure 41.3 (b). We plot here the coordinate and momentum of the outer electron whenever the inner particle hits the nucleus, i.e., r_1 or $r_2 = 0$. As the unstructured gray region of the Poincaré section for small r_1 illustrates, the dynamics is chaotic whenever the outer electron is close to the origin during a collision. Conversely, regular motions dominate whenever the outer electron is far from the nucleus. As one of the electrons escapes for almost any starting condition, the system is unbounded: one electron (say electron 1) can escape, with an arbitrary amount of kinetic energy taken by the fugative. The remaining electron is trapped in a Kepler ellipse with total energy in the range $[-1, -\infty]$. There is no energy barrier which would separate the bound from the unbound regions of the phase space. From general kinematic arguments one deduces that the outer electron will not return when $p_1 > 0$, $r_2 \leq 2$ at $p_2 = 0$, the turning point of the inner electron. Only if the two electrons approach the nucleus almost symmetrically along the line $r_1 = r_2$, and pass close to the triple collision can the momentum transfer between the electrons be large enough to kick one of the particles out completely. In other words, the electron escape originates from the near triple collisions.

The collinear helium dynamics has some important properties which we now list.

41.2.1 Reflection symmetry

The Hamiltonian (7.9) is invariant with respect to electron–electron exchange; this symmetry corresponds to the mirror symmetry of the potential along the line $r_1 = r_2$, figure 41.4. As a consequence, we can restrict ourselves to the dynamics in the *fundamental domain* $r_1 \geq r_2$ and treat a crossing

of the diagonal $r_1 = r_2$ as a hard wall reflection. The dynamics in the full domain can then be reconstructed by unfolding the trajectory through back-reflections. As explained in chapter 22, the dynamics in the fundamental domain is the key to the factorization of spectral determinants, to be implemented here in (41.15). Note also the similarity between the fundamental domain of the collinear potential figure 41.4, and the fundamental domain figure 11.6 (b) in the 3–disk system, a simpler problem with the same binary symbolic dynamics.

collinear
helium!symbolic
dynamics
symbolic
dynamics!binary!collinear
helium
binary!symbolic
dynamics!collinear
helium

in depth:
sect. 22.6, p. 442

41.2.2 Symbolic dynamics

We have already made the claim that the triple collisions render the collinear helium fully chaotic. We have no proof of the assertion, but the analysis of the symbolic dynamics lends further credence to the claim.

The potential in (41.1) forms a ridge along the line $r_1 = r_2$. One can show that a trajectory passing the ridge must go through at least one two-body collision $r_1 = 0$ or $r_2 = 0$ before coming back to the diagonal $r_1 = r_2$. This suggests a *binary* symbolic dynamics corresponding to the dynamics in the fundamental domain $r_1 \geq r_2$; the symbolic dynamics is linked to the Poincaré map $r_2 = 0$ and the symbols 0 and 1 are defined as

0: if the trajectory is not reflected from the line $r_1 = r_2$ between two collisions with the nucleus $r_2 = 0$;

1: if a trajectory is reflected from the line $r_1 = r_2$ between two collisions with the nucleus $r_2 = 0$.

Empirically, the symbolic dynamics is complete for a Poincaré map in the fundamental domain, i.e., there exists a one-to-one correspondence between binary symbol sequences and collinear trajectories in the fundamental domain, with exception of the $\overline{0}$ cycle.

41.2.3 Periodic orbits

The existence of a binary symbolic dynamics makes it easy to count the number of periodic orbits in the fundamental domain, as in sect. 13.5.2. However, mere existence of these cycles does not suffice to calculate semiclassical spectral determinants. We need to determine their phase space trajectories and calculate their periods, topological indices and stabilities. A restriction of the periodic orbit search to a suitable Poincaré surface of section, e.g. $r_2 = 0$ or $r_1 = r_2$, leaves us in general with a 2-dimensional search. Methods to find periodic orbits in multi-dimensional spaces have been

libration orbit
self-retracing cycle

described in chapter 17. They depend sensitively on good starting guesses. A systematic search for all orbits can be achieved only after combining multi-dimensional Newton methods with interpolation algorithms based on the binary symbolic dynamics phase space partitioning(see sect. 17.6.3) . All cycles up to symbol length 16 (some 8000 primitive cycles) have been computed by such methods, with some examples shown in figure 41.5. All numerical evidence indicates that the dynamics of collinear helium is hyperbolic, and that all periodic orbits are unstable.

⇓PRELIMINARY
⇑PRELIMINARY
into remarks: cite Tanner

Note that the fixed point $\overline{0}$ cycle is not in this list. The $\overline{0}$ cycle would correspond to the situation where the outer electron sits at rest infinitely far from the nucleus while the inner electron bounces back and forth into the nucleus. The orbit is the limiting case of an electron escaping to infinity with zero kinetic energy. The orbit is in the regular (i.e., separable) limit of the dynamics and is thus marginally stable. The existence of this orbit is also related to intermittent behavior generating the quasi–regular dynamics for large r_1 that we have already noted in figure 41.3 (b).

Search algorithm for an arbitrary periodic orbit is quite cumbersome to program. There is, however, a class of periodic orbits, orbits with symmetries, which can be easily found by a one-parameter search. The only symmetry left for the dynamics in the fundamental domain is time reversal symmetry; a time reversal symmetric periodic orbit is an orbit whose trajectory in phase space is mapped onto itself when changing $(p_1, p_2) \to (-p_1, -p_2)$, by reversing the direction of the momentum of the orbit. Such an orbit must be a "libration" [1] or self-retracing cycle, an orbit that runs back and forth along the same path in the (r_1, r_2) plane. The cycles $\overline{1}$, $\overline{01}$ and $\overline{001}$ in figure 41.5 are examples of self-retracing cycles. Luckily, the shortest cycles that we desire most ardently have this symmetry.

buscar en la red: for example "Breve dictionario del argentino exquisito" Adolfo Bioy Cesares, for "capicua"

Why is this observation helpful? A self-retracing cycle must start perpendicular to the boundary of the fundamental domain, that is, on either of the axis $r_2 = 0$ or $r_1 = r_2$, or on the potential boundary $-\frac{2}{r_1}-\frac{2}{r_2}+\frac{1'}{r_1+r_2} = -1$. By shooting off trajectories perpendicular to the boundaries and monitoring the orbits returning to the boundary with the right symbol length we will find time reversal symmetric cycles by varying the starting point on the boundary as the only parameter. But how can we tell whether a given cycle is self-retracing or not? All the relevant information is contained in the itineraries; a cycle is self-retracing if its itinerary is invariant under time reversal symmetry (i.e., read backwards) and a suitable number of cyclic permutations. All binary strings up to length 5 fulfill this condition. The symbolic dynamics contains even more information; we can tell at which boundary the total reflection occurs. One finds that an orbit starts out perpendicular

- to the diagonal $r_1 = r_2$ if the itinerary is time reversal invariant and has an odd number of 1's; an example is the cycle $\overline{001}$ in figure 41.5;

[1] Tanner: Explain that much earlier

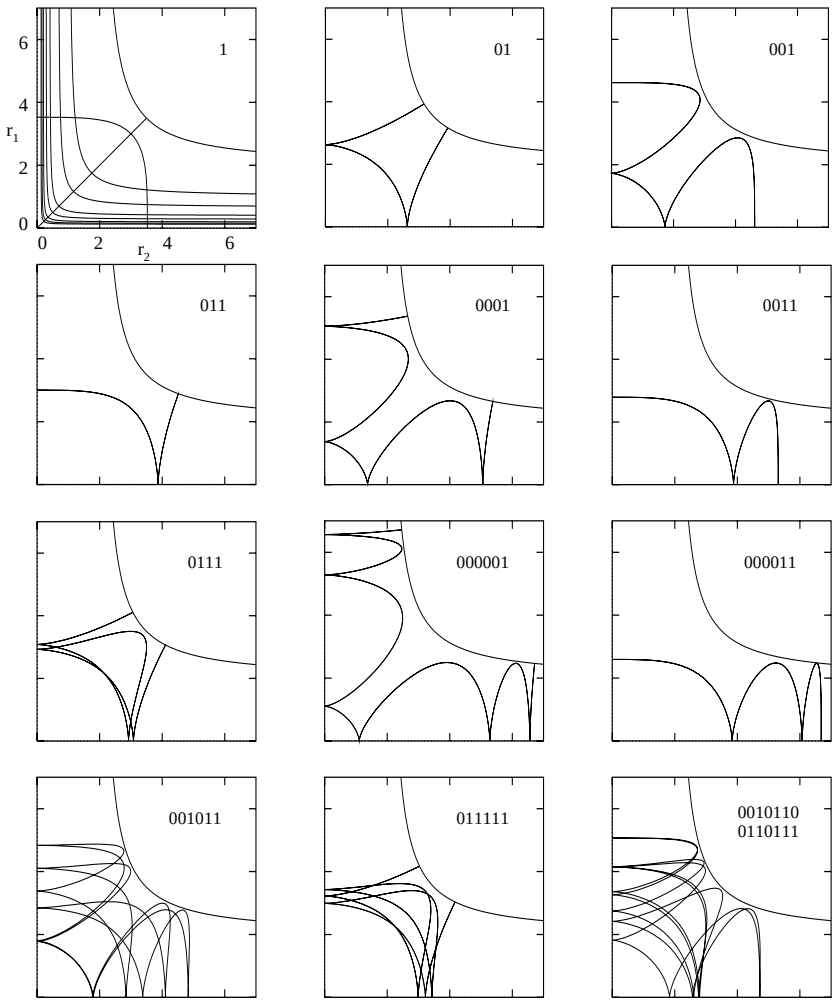

Figure 41.5: Some of the shortest cycles in collinear helium. The classical collinear electron motion is bounded by the potential barrier $-1 = -2/r_1 - 2/r_2 + 1/(r_1 + r_2)$ and the condition $r_i \geq 0$. The orbits are shown in the full r_1–r_2 domain, the itineraries refers to the dynamics in the $r_1 \geq r_2$ fundamental domain. The last figure, the 14-cycle 00101100110111, is an example of a typical cycle with no symmetry.

- to the axis $r_2 = 0$ if the itinerary is time reversal invariant and has an even number of symbols; an example is the cycle $\overline{0011}$ in figure 41.5;

- to the potential boundary if the itinerary is time reversal invariant and has an odd number of symbols; an example is the cycle $\overline{011}$ in figure 41.5.

where are these cycles in figure 41.5?

All cycles up to symbol length 5 are time reversal invariant, the first two non-time reversal symmetric cycles are cycles $\overline{001011}$ and $\overline{001101}$ in figure 41.5. Their determination would require a two-parameter search. The two cycles are mapped onto each other by time reversal symmetry, i.e., they have the same trace in the r_1–r_2 plane, but they trace out distinct cycles in the full phase space.

mention that 001101 is not in Fig. 25.5

We are ready to integrate trajectories for classical collinear helium with the help of the equations of motions (7.18) and to find all cycles up to length 5. There is only one thing not yet in place; we need the governing equations for the matrix elements of the fundamental matrix along a trajectory in order to calculate stability indices. We will provide the main equations in the next section, with the details of the derivation relegated to the appendix D.2. [2]

41.5
page 794

41.3 Local coordinates, fundamental matrix

In this section, we will derive the equations of motion for the fundamental matrix along a collinear helium trajectory. The fundamental matrix is 4-dimensional; the two trivial eigenvectors corresponding to the conservation of energy and displacements along a trajectory can, however, be projected out by suitable orthogonal coordinates transformations, see appendix D. We will give the transformation to local coordinates explicitly, here for the regularized coordinates (7.16), and state the resulting equations of motion for the reduced $[2 \times 2]$ fundamental matrix.

The vector locally parallel to the trajectory is pointing in the direction of the phase space velocity (5.7)

$$v_m = \dot{x}_m(t) = \omega_{mn} \frac{\partial H}{\partial x_n} = (H_{P_1}, H_{P_2}, -H_{Q_1}, -H_{Q_2})^T,$$

with $H_{Q_i} = \frac{\partial H}{\partial Q_i}$, and $H_{P_i} = \frac{\partial H}{\partial P_i}$, $i = 1,2$. The vector perpendicular to a trajectory $x(t) = (Q_1(t), Q_2(t), P_1(t), P_2(t))$ and to the energy manifold is given by the gradient of the Hamiltonian (7.17)

$$\gamma = \nabla H = (H_{Q_1}, H_{Q_2}, H_{P_1}, H_{P_2})^T .$$

[2] Tanner: Have a look at that appendix

By symmetry $v_m\gamma_m = \omega_{mn}\frac{\partial H}{\partial x_n}\frac{\partial H}{\partial x_m} = 0$, so the two vectors are orthogonal.

Next, we consider the orthogonal matrix

$$\begin{aligned}\mathbf{O} &= (\gamma_1, \gamma_2, \gamma/R, v) \qquad (41.5)\\ &= \begin{pmatrix} -H_{P_2}/R & H_{Q_2} & H_{Q_1}/R & H_{P_1} \\ H_{P_1}/R & -H_{Q_1} & H_{Q_2}/R & H_{P_2} \\ -H_{Q_2}/R & -H_{P_2} & H_{P_1}/R & -H_{Q_1} \\ H_{Q_1}/R & H_{P_1} & H_{P_2}/R & -H_{Q_2} \end{pmatrix}\end{aligned}$$

with $R = |\nabla H|^2 = (H_{Q_1}^2 + H_{Q_2}^2 + H_{P_1}^2 + H_{P_2}^2)$, which provides a transformation to local phase space coordinates centered on the trajectory $x(t)$ along the two vectors (γ, v). The vectors $\gamma_{1,2}$ are phase space vectors perpendicular to the trajectory and to the energy manifold in the 4-dimensional phase space of collinear helium. The fundamental matrix (4.6) rotated to the local coordinate system by $\mathbf{O}$ then has the form

41.6
page 795

Gregor had a σ here, maybe a symplectic form ω is missing, recheck

$$\mathbf{m} = \begin{pmatrix} m_{11} & m_{12} & * & 0 \\ m_{21} & m_{22} & * & 0 \\ 0 & 0 & 1 & 0 \\ * & * & * & 1 \end{pmatrix}, \quad M = \mathbf{O^T m O}$$

The linearized motion perpendicular to the trajectory on the energy manifold is described by the $[2 \times 2]$ matrix $\mathbf{m}$; the 'trivial' directions correspond to unit eigenvalues on the diagonal in the 3rd and 4th column and row.

The equations of motion for the reduced fundamental matrix $\mathbf{m}$ are given by

$$\dot{\mathbf{m}} = \mathbf{l}(t)\mathbf{m}(t), \qquad (41.6)$$

with $\mathbf{m}(0) = \mathbf{1}$. The matrix $\mathbf{l}$ depends on the trajectory in phase space and has the form

$$\mathbf{l} = \begin{pmatrix} l_{11} & l_{12} & * & 0 \\ l_{21} & l_{22} & * & 0 \\ 0 & 0 & 0 & 0 \\ * & * & * & 0 \end{pmatrix},$$

where the relevant matrix elements l_{ij} are given by

$$\begin{aligned} l_{11} &= \frac{1}{R}[2H_{Q_1Q_2}(H_{Q_2}H_{P_1} + H_{Q_1}H_{P_2}) \qquad (41.7)\\ &\quad +(H_{Q_1}H_{P_1} - H_{Q_2}H_{P_2})(H_{Q_1Q_1} - H_{Q_2Q_2} - H_{P_1P_1} + H_{P_2P_2})] \\ l_{12} &= -2H_{Q_1Q_2}(H_{Q_1}H_{Q_2} - H_{P_1}H_{P_2}) \\ &\quad +(H_{Q_1}^2 + H_{P_2}^2)(H_{Q_2Q_2} + H_{P_1P_1}) + (H_{Q_2}^2 + H_{P_1}^2)(H_{Q_1Q_1} + H_{P_2P_2}) \\ l_{21} &= \frac{1}{R^2}[2(H_{Q_1P_2} + H_{Q_2P_1})(H_{Q_2}H_{P_1} + H_{Q_1}H_{P_8}) \\ &\quad -(H_{P_1}^2 + H_{P_2}^2)(H_{Q_1Q_1} + H_{Q_2Q_2}) - (H_{Q_1}^2 + H_{Q_2}^2)(H_{P_1P_1} + H_{P_2P_2})] \\ l_{22} &= -l_{11}\,. \end{aligned}$$

action!relation to period
period!relation to action

p	$S_p/2\pi$	$\ln \lvert\Lambda_p\rvert$	σ_p	m_p
1	1.82900	0.6012	0.5393	2
01	3.61825	1.8622	1.0918	4
001	5.32615	3.4287	1.6402	6
011	5.39451	1.8603	1.6117	6
0001	6.96677	4.4378	2.1710	8
0011	7.04134	2.3417	2.1327	8
0111	7.25849	3.1124	2.1705	8
00001	8.56618	5.1100	2.6919	10
00011	8.64306	2.7207	2.6478	10
00101	8.93700	5.1562	2.7291	10
00111	8.94619	4.5932	2.7173	10
01011	9.02689	4.1765	2.7140	10
01111	9.07179	3.3424	2.6989	10
000001	10.13872	5.6047	3.2073	12
000011	10.21673	3.0323	3.1594	12
000101	10.57067	6.1393	3.2591	12
000111	10.57628	5.6766	3.2495	12
001011	10.70698	5.3251	3.2519	12
001101	10.70698	5.3251	3.2519	12
001111	10.74303	4.3317	3.2332	12
010111	10.87855	5.0002	3.2626	12
011111	10.91015	4.2408	3.2467	12

Table 41.1: Action S_p (in units of 2π), Lyapunov exponent $|\Lambda_p|/T_p$ for the motion in the collinear plane, winding number σ_p for the motion perpendicular to the collinear plane, and the topological index m_p for all fundamental domain cycles up to topological length 6.

Here $H_{Q_iQ_j}$, $H_{P_iP_j}$, i, $j = 1, 2$ are the second partial derivatives of H with respect to the coordinates Q_i, P_i, evaluated at the phase space coordinate of the classical trajectory. [3]

[4]

41.4 Getting ready

Now everything is in place: the regularized equations of motion can be implemented in a Runge–Kutta or any other integration scheme to calculate trajectories. We have a symbolic dynamics and know how many cycles there are and how to find them (at least up to symbol length 5). We know how to compute the fundamental matrix whose eigenvalues enter the semiclassical spectral determinant (36.13). By (34.17) the action S_p is proportional to the period of the orbit, $S_p = 2T_p$.

There is, however, still a slight complication. Collinear helium is an invariant 4-dimensional subspace of the full helium phase space. If we

[3] Dorte: uforstaaeligt!
[4] Tanner: Check if σ in table 41.3 in multiples of π or 2π.

Bohr!helium
Rydberg series

restrict the dynamics to angular momentum equal zero, we are left with 6 phase space coordinates. That is not a problem when computing periodic orbits, they are oblivious to the other dimensions. However, the fundamental matrix does pick up extra contributions. When we calculate the fundamental matrix for the full problem, we must also allow for displacements out of the collinear plane, so the full fundamental matrix for dynamics for $L = 0$ angular momentum is 6 dimensional. Fortunately, the linearized dynamics in and off the collinear helium subspace decouple, and the fundamental matrix can be written in terms of two distinct $[2 \times 2]$ matrices, with trivial eigendirections providing the remaining two dimensions. The submatrix related to displacements off the linear configuration characterizes the linearized dynamics in the additional degree of freedom, the Θ-coordinate in figure 41.1. It turns out that the linearized dynamics in the Θ coordinate is stable, corresponding to a bending type motion of the two electrons. We will need the stability exponents for all degrees of freedom in evaluating the semiclassical spectral determinant in sect. 41.5.

The numerical values of the actions, stability exponents, stability angles, and topological indices for the shortest cycles are listed in table 41.3. These numbers, needed for the semiclassical quantization implemented in the next section, an also be helpful in checking your own calculations.

41.5 Semiclassical quantization of collinear helium

Before we get down to a serious calculation of the helium quantum energy levels let us have a brief look at the overall structure of the spectrum. This will give us a preliminary feel for which parts of the helium spectrum are accessible with the help of our collinear model – and which are not. In order to keep the discussion as simple as possible and to concentrate on the semiclassical aspects of our calculations we offer here only a rough overview. For a guide to more detailed accounts see remark 41.4.

41.5.1 Structure of helium spectrum

We start by recalling Bohr's formula for the spectrum of hydrogen like one-electron atoms. The eigenenergies form a Rydberg series

$$E_N = -\frac{e^4 m_e}{\hbar^2}\frac{Z^2}{2N^2}\,, \tag{41.8}$$

where Ze is the charge of the nucleus and m_e is the mass of the electron. Through the rest of this chapter we adopt the atomic units $e = m_e = \hbar = 1$.

The simplest model for the helium spectrum is obtained by treating the two electrons as independent particles moving in the potential of the nucleus neglecting the electron–electron interaction. Both electrons are then bound

in hydrogen like states; the inner electron will see a charge $Z = 2$, screening at the same time the nucleus, the outer electron will move in a Coulomb potential with effective charge $Z-1 = 1$. In this way obtain a first estimate for the total energy

$$E_{N,n} = -\frac{2}{N^2} - \frac{1}{2n^2} \qquad \text{with} \quad n > N. \tag{41.9}$$

This double Rydberg formula contains already most of the information we need to understand the basic structure of the spectrum. The (correct) ionizations thresholds $E_N = -\frac{2}{N^2}$ are obtained in the limit $n \to \infty$, yielding the ground and excited states of the helium ion He^+. We will therefore refer to N as the principal quantum number. We also see that all states $E_{N,n}$ with $N \geq 2$ lie above the first ionization threshold for $N = 1$. As soon as we switch on electron-electron interaction these states are no longer bound states; they turn into resonant states which decay into a bound state of the helium ion and a free outer electron. This might not come as a big surprise if we have the classical analysis of the previous section in mind: we already found that one of the classical electrons will almost always escape after some finite time. More remarkable is the fact that the first, $N = 1$ series consists of true bound states for all n, an effect which can only be understood by quantum arguments.

The hydrogen-like quantum energies (41.8) are highly degenerate; states with different angular momentum but the same principal quantum number N share the same energy. We recall from basic quantum mechanics of hydrogen atom that the possible angular momenta for a given N span $l = 0, 1 \ldots N-1$. How does that affect the helium case? Total angular momentum L for the helium three-body problem is conserved. The collinear helium is a subspace of the classical phase space for $L = 0$; we thus expect that we can only quantize helium states corresponding to the total angular momentum zero, a subspectrum of the full helium spectrum. Going back to our crude estimate (41.9) we may now attribute angular momenta to the two independent electrons, l_1 and l_2 say. In order to obtain total angular momentum $L = 0$ we need $l_1 = l_2 = l$ and $l_{z1} = -l_{z2}$, that is, there are N different states corresponding to $L = 0$ for fixed quantum numbers N, n. That means that we expect N different Rydberg series converging to each ionization threshold $E_N = -2/N^2$. This is indeed the case and the N different series can be identified also in the exact helium quantum spectrum, see figure 41.6. The degeneracies between the different N Rydberg series corresponding to the same principal quantum number N, are removed by the electron-electron interaction. We thus already have a rather good idea of the coarse structure of the spectrum.

In the next step, we may even speculate which parts of the $L = 0$ spectrum can be reproduced by the semiclassical quantization of collinear helium. In the collinear helium, both classical electrons move back and forth along a common axis through the nucleus, so each has zero angular momentum. We therefore expect that collinear helium describes the Rydberg series with $l = l_1 = l_2 = 0$. These series are the energetically lowest states

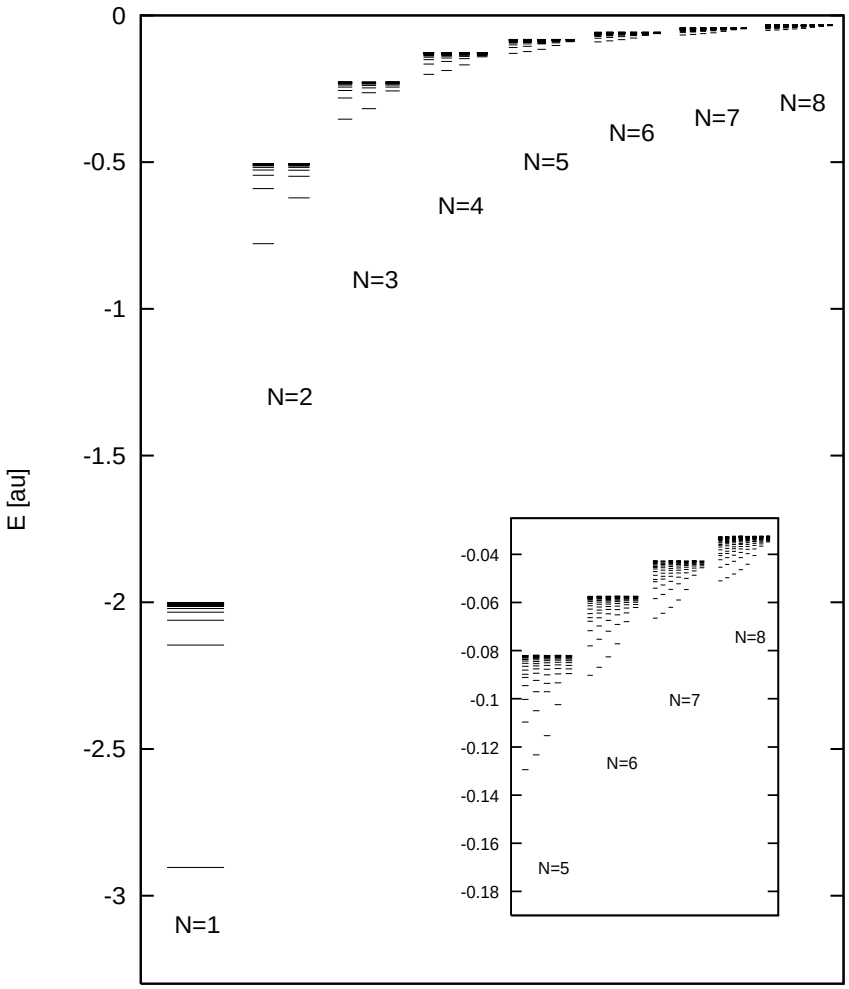

Figure 41.6: The exact quantum helium spectrum for $L = 0$. The energy levels denoted [5] by bars have been obtained from full 3-dimensional quantum calculations [41.3].

Dorte: ulaeseligt

semiclassical!spectral determinant!collinear helium
staircase!mean eigenvalue density

for fixed (N, n), corresponding to the Rydberg series on the outermost left side of the spectrum in figure 41.6. We will see in the next section that this is indeed the case and that the collinear model holds down to the $N = 1$ bound state series, including even the ground state of helium! We will also find a semiclassical quantum number corresponding to the angular momentum l and show that the collinear model describes states for moderate angular momentum l as long as $l \ll N$. .

☞ remark 41.4

41.5.2 Semiclassical spectral determinant for collinear helium

Nothing but lassitude can stop us now from calculating our first semiclassical eigenvalues. The only thing left to do is to set up the spectral determinant in terms of the periodic orbits of collinear helium and to write out the first few terms of its cycle expansion with the help of the binary symbolic dynamics. The semiclassical spectral determinant (36.13) has been written as product over all cycles of the classical systems. The energy dependence in collinear helium enters the classical dynamics only through simple scaling transformations described in sect. 7.3.1 which makes it possible to write the semiclassical spectral determinant in the form

$$\det\left(\hat{H}-E\right)_{sc} = \exp\left(-\sum_{p}\sum_{r=1}^{\infty}\frac{1}{r}\frac{e^{ir(sS_p-m_p\frac{\pi}{2})}}{(-\det\left(1-M_{p\perp}^{r}\right))^{1/2}|\det\left(1-M_{p\parallel}^{r}\right)|^{1/2}}\right), \quad (41.10)$$

replace by k? then $k \to \ell$ elsewhere

with the energy dependence absorbed into the variable

$$s = \frac{e^2}{\hbar}\sqrt{\frac{m_e}{-E}},$$

obtained by using the scaling relation (41.2) for the action. As explained in sect. 41.3, the fact that the $[4 \times 4]$ fundamental matrix decouples into two $[2 \times 2]$ submatrices corresponding to the dynamics *in* the collinear space and *perpendicular* to it makes it possible to write the denominator in terms of a product of two determinants. Stable and unstable degrees of freedom enter the trace formula in different ways, (see the discussion in sect. **??**) [6] [7] reflected by the absence of the modulus sign and the minus sign in front of $\det\left(1 - M_{\perp}\right)$. The topological index m_p corresponds to the unstable dynamics in the collinear plane. Note that the factor $e^{i\pi\bar{N}(E)}$ present in (36.13) is absent in (41.10). Collinear helium is an open system, i.e., the eigenenergies are resonances corresponding to the complex zeros of the semiclassical spectral determinant and the mean energy staircase $\bar{N}(E)$ not defined. [8] In order to obtain a spectral determinant as an infinite product of the form (36.19) we may proceed as in (15.10) by expanding the determinants in (41.10) in terms of the eigenvalues of the corresponding

⇓PRELIMINARY
⇑PRELIMINARY

[6] Dorte: sect. **??**hat??
[7] Tanner: reference
[8] Tanner: Make reference to Andreas chapter

fundamental matrices. The matrix representing displacements perpendicular to the collinear space has eigenvalues of the form $\exp(\pm 2\pi i\sigma)$, reflecting stable linearized dynamics. σ is the full winding number along the orbit in the stable degree of freedom, multiplicative under multiple repetitions of this orbit , see sect. **??**. [9] The eigenvalues corresponding to the unstable dynamics along the collinear axis are paired as $\{\Lambda, 1/\Lambda\}$ with $|\Lambda| > 1$ and real. As in (15.10) and (36.19) we may thus write

⇓PRIVATE
⇑PRIVATE

$$\begin{aligned}
&\left[-\det\left(1-M_\perp^r\right)\left|\det\left(1-M_\parallel^r\right)\right|\right]^{-1/2} \qquad (41.11)\\
&= \left[-(1-\Lambda^r)(1-\Lambda^{-r})|(1-e^{2\pi i r\sigma})(1-e^{-2\pi i r\sigma})\right]^{-1/2}\\
&= \sum_{k,\ell=0}^{\infty} \frac{1}{|\Lambda^r|^{1/2}\Lambda^{rk}} e^{-ir(\ell+1/2)\sigma}\,.
\end{aligned}$$

The $\pm$ sign corresponds to the hyperbolic/inverse hyperbolic periodic orbits with positive/negative eigenvalues Λ. [10] Using the relation (41.12) we see that the sum over r in (41.10) is the expansion of the logarithm, so the semiclassical spectral determinant can be rewritten as a product over dynamical zeta functions, as in (15.10): [11]

problem: same as Maslov

$$\det\left(\hat{H}-E\right)_{sc} = \prod_{k=0}^{\infty}\prod_{m=0}^{\infty}\zeta_{k,m}^{-1} = \prod_{k=0}^{\infty}\prod_{m=0}^{\infty}\prod_{p}(1-t_p^{(k,m)})\,, \qquad (41.12)$$

where the cycle weights are given by

$$t_p^{(k,m)} = \frac{1}{|\Lambda|^{1/2}\Lambda^k} e^{i\left(sS_p - m_p\frac{\pi}{2} - 4\pi(\ell+1/2)\sigma_p\right)}\,, \qquad (41.13)$$

and m_p is the topological index for the motion in the collinear plane which equals twice the topological length of the cycle. [12] The two independent directions perpendicular to the collinear axis lead to a twofold degeneracy in this degree of freedom which accounts for an additional factor 2 in front of the winding number σ. The values for the actions, winding numbers and stability indices of the shortest cycles in collinear helium are listed in table 41.3.

Gregor, I have changed to Lyapunov exponent $\lambda_p = \log|\Lambda_p|/T$, rather than stability exponent $\lambda_p = \log|\Lambda_p|$, for consistency with the rest of the text

The integer indices ℓ and k play very different roles in the semiclassical spectral determinant (41.12). A linearized approximation of the flow along a cycle corresponds to a harmonic approximation of the potential in the vicinity of the trajectory. Stable motion corresponds to a harmonic oscillator potential, unstable motion to an inverted harmonic oscillator.

[9] Tanner: Ref to section about isolated stable orbits.
[10] Tanner: Discuss invers/hyperbolic orbit, even/odd maslov; ref to gutzwiller chapter.
[11] Mason: It states, "Using the relation (25.19)" to get equation... (25.19). Most likely possibility is that the first 21.19 should be 21.xx for some other xx.
[12] Tanner: Explain why

The index ℓ which contributes as a phase to the cycle weights in the dynamical zeta functions can therefore be interpreted as a harmonic oscillator quantum number; it corresponds to vibrational modes in the Θ coordinate and can in our simplified picture developed in sect. 41.5.1 be related to the quantum number $l = l_1 = l_2$ representing the single particle angular momenta. Every distinct ℓ value corresponds to a full spectrum which we obtain from the zeros of the semiclassical spectral determinant $1/\zeta_\ell$ keeping ℓ fixed. The harmonic oscillator approximation will eventually break down with increasing off-line excitations and thus increasing ℓ. The index k corresponds to 'excitations' along the unstable direction and can be identified with local resonances of the inverted harmonic oscillator centered on the given orbit. [13] The cycle contributions $t_p^{(k,m)}$ decrease exponentially with increasing k. Higher k terms in an expansion of the determinant give corrections which become important only for large negative imaginary s values. As we are interested only in the leading zeros of (41.12), i.e., the zeros closest to the real energy axis, it is sufficient to take only the $k = 0$ terms into account.

cross reference

Next, let us have a look at the discrete symmetries discussed in sect. 41.2. Collinear helium has a C_2 symmetry as it is invariant under reflection across the $r_1 = r_2$ line corresponding to the electron-electron exchange symmetry. As explained in sects. 22.1.2 and 22.5, we may use this symmetry to factorize the semiclassical spectral determinant. The spectrum corresponding to the states symmetric or antisymmetric with respect to reflection can be obtained by writing the dynamical zeta functions in the symmetry factorized form

$$1/\zeta^{(\ell)} = \prod_a (1 - t_a)^2 \prod_{\tilde{s}} (1 - t_{\tilde{s}}^2)\,. \tag{41.14}$$

say m dependence implicit in $t_a = t_a^{(0,\ell)}$ as defined in (28.14a)

Here, the first product is taken over all asymmetric prime cycles, i.e., cycles that are not self-dual under the C_2 symmetry. Such cycles come in pairs, as two equivalent orbits are mapped into each other by the symmetry transformation. The second product runs over all self-dual cycles; these orbits cross the axis $r_1 = r_2$ twice at a right angle. The self-dual cycles close in the fundamental domain $r_1 \leq r_2$ already at half the period compared to the orbit in the full domain, and the cycle weights $t_{\tilde{s}}$ in (41.14) are the weights of fundamental domain cycles. The C_2 symmetry now leads to the factorization of (41.14) $1/\zeta = \zeta_+^{-1}\zeta_-^{-1}$, with

$$\begin{aligned} 1/\zeta_+^{(\ell)} &= \prod_a (1 - t_a) \prod_{\tilde{s}} (1 - t_{\tilde{s}})\,, \\ 1/\zeta_-^{(\ell)} &= \prod_a (1 - t_a) \prod_{\tilde{s}} (1 + t_{\tilde{s}})\,, \end{aligned} \tag{41.15}$$

setting $k = 0$ in what follows. The symmetric subspace resonances are given by the zeros of $1/\zeta_+^{(\ell)}$, antisymmetric resonances by the zeros of $1/\zeta_-^{(\ell)}$, with

[13] Tanner: Reference Gabor chapter

the two dynamical zeta functions defined as products over orbits in the fundamental domain. The symmetry properties of an orbit can be read off directly from its symbol sequence, as explained in sect. 41.2. An orbit with an odd number of 1's in the itinerary is self-dual under the C_2 symmetry and enters the spectral determinant in (41.15) with a negative or a positive sign, depending on the symmetry subspace under consideration.

41.5.3 Cycle expansion results

So far we have established a factorized form of the semiclassical spectral determinant and have thereby picked up two *good quantum numbers*; the quantum number m has been identified with an excitation of the bending vibrations, the exchange symmetry quantum number ± 1 corresponds to states being symmetric or antisymmetric with respect to the electron-electron exchange. We may now start writing down the binary cycle expansion (18.5) and determine the zeros of spectral determinant. There is, however, still another problem: there is no cycle 0 in the collinear helium. The symbol sequence $\overline{0}$ corresponds to the limit of an outer electron fixed with zero kinetic energy at $r_1 = \infty$, the inner electron bouncing back and forth into the singularity at the origin. This introduces intermittency in our system, a problem discussed in chapter 21. We note that the behavior of cycles going far out in the channel r_1 or $r_2 \to \infty$ is very different from those staying in the near core region. A cycle expansion using the binary alphabet reproduces states where both electrons are localized in the near core regions: these are the lowest states in each Rydberg series. The states converging to the various ionization thresholds $E_N = -2/N^2$ correspond to eigenfunctions where the wave function of the outer electron is stretched far out into the ionization channel $r_1, r_2 \to \infty$. To include those states, we have to deal with the dynamics in the limit of large r_1, r_2. This turns out to be equivalent to switching to a symbolic dynamics with an infinite alphabetdiscussed in sect. 21.3.1, a step beyond our ambition horizon right now. With this observation in mind, we may write the cycle expansion (....) for a binary alphabet without the $\overline{0}$ cycle as

⇓PRELIMINARY
⇑PRELIMINARY
☞ remark 41.5
replace by the intermittency table

$$
\begin{aligned}
1/\zeta^{\ell}(s) = \quad 1 \quad & -t_1^{(\ell)} - t_{01}^{(\ell)} - [t_{001}^{(\ell)} + t_{011}^{(\ell)} - t_{01}^{(\ell)} t_1^{(\ell)}] \\
& -[t_{0001}^{(\ell)} + t_{0011}^{(\ell)} - t_{001}^{(\ell)} t_1^{(\ell)} + t_{0111}^{(\ell)} - t_{011}^{(\ell)} t_1^{(\ell)}] - \ldots
\end{aligned} \tag{41.16}
$$

The weights $t_p^{(\ell)}$ are given in (41.12), with contributions of orbits and composite orbits of the same total symbol length collected within square brackets. The cycle expansion depends only on the classical actions, stability indices and winding numbers, given for orbits up to length 6 in table 41.3. To get reacquainted with the cycle expansion formula (41.16), consider a truncation of the series after the first term

$$
1/\zeta^{(\ell)}(s) \approx 1 - t_1 \,.
$$

N	n	$j=1$	$j=4$	$j=8$	$j=12$	$j=16$	$-E_{\rm qm}$
1	1	3.0970	2.9692	2.9001	2.9390	2.9248	2.9037
2	2	0.8044	0.7714	0.7744	0.7730	0.7727	0.7779
2	3	—	0.5698	0.5906	0.5916	0.5902	0.5899
2	4	—	—	—	0.5383	0.5429	0.5449
3	3	0.3622	0.3472	0.3543	0.3535	0.3503	0.3535
3	4	—	—	0.2812	0.2808	0.2808	0.2811
3	5	—	—	0.2550	0.2561	0.2559	0.2560
3	6	—	—	—	0.2416	0.2433	0.2438
4	4	0.2050	0.1962	0.1980	0.2004	0.2012	0.2010
4	5	—	0.1655	0.1650	0.1654	0.1657	0.1657
4	6	—	—	0.1508	0.1505	0.1507	0.1508
4	7	—	—	0.1413	0.1426	0.1426	0.1426

Table 41.2: Collinear helium, real part of the symmetric subspace resonances obtained by a cycle expansion (41.16) up to cycle length j. The exact quantum energies [41.3] are in the last column. The states are labeled by their principal quantum numbers. A dash as an entry indicates a missing zero at that level of approximation.

The quantization condition $1/\zeta^{(\ell)}(s)=0$ leads to

$$E_{m,N}=-\frac{(S_1/2\pi)^2}{[m+\frac{1}{2}+2(N+\frac{1}{2})\sigma_1]^2}, \qquad m,N=0,1,2,\dots\ , \tag{41.17}$$

with $S_1/2\pi = 1.8290$ for the action and $\sigma_1 = 0.5393$ for the winding number, see table 41.3, the 1 cycle in the fundamental domain. This cycle can be described as the *asymmetric stretch* orbit, see figure 41.5. The additional quantum number N in (41.17) corresponds to the principal quantum number defined in sect. 41.5.1. The states described by the quantization condition (41.17) are those centered closest to the nucleus and correspond therefore to the lowest states in each Rydberg series (for a fixed m and N values), in figure 41.6. The simple formula (41.17) gives already a rather good estimate for the ground state of helium! Results obtained from (41.17) are tabulated in table 41.2, see the 3rd column under $j=1$ and the comparison with the full quantum calculations.

In order to obtain higher excited quantum states, we need to include more orbits in the cycle expansion (41.16), covering more of the phase space dynamics further away from the center. Taking longer and longer cycles into account, we indeed reveal more and more states in each N-series for fixed m. This is illustrated by the data listed in table 41.2 for symmetric states obtained from truncations of the cycle expansion of $1/\zeta_+$.

41.7
page 795

Results of the same quality are obtained for antisymmetric states by calculating the zeros of [14] $1/\zeta_-^{(\ell)}$. Repeating the calculation with $\ell=1$ or higher in (41.15) reveals states in the Rydberg series which are to the right of the energetically lowest series in figure 41.6.

[14] Dorte: ulaesligt

Hopf, Heinz

Commentary

Remark 41.1 Sources. The full 3-dimensional Hamiltonian after elimination of the center of mass coordinates, and an account of the finite nucleus mass effects is given in ref. [41.2]. The general two–body collision regularizing Kustaanheimo–Stiefel transformation [41.5], a generalization of Levi-Civita's [41.13] Pauli matrix two–body collision regularization for motion in a plane, is due to Kustaanheimo [41.12] who realized that the correct higher-dimensional generalization of the "square root removal" trick (7.14), by introducing a vector Q with property $r = |Q|^2$, is the same as Dirac's trick of getting linear equation for spin 1/2 fermions by means of spinors. Vector spaces equipped with a product and a known satisfy $|Q \cdot Q| = |Q|^2$ define *normed algebras*. They appear in various physical applications - as quaternions, octonions, spinors. The technique was originally developed in celestial mechanics [41.6] to obtain numerically stable solutions for planetary motions. The basic idea was in place as early as 1931, when H. Hopf [41.14] used a KS transformation in order to illustrate a Hopf's invariant. The KS transformation for the collinear helium was introduced in ref. [41.2].

Remark 41.2 Complete binary symbolic dynamics. No stable periodic orbit and no exception to the binary symbolic dynamics of the collinear helium cycles have been found in numerical investigations. A proof that all cycles are unstable, that they are uniquely labeled by the binary symbolic dynamcis, and that this dynamics is complete is, however, still missing. The conjectured Markov partition of the phase space is given by the triple collision manifold, i.e., by those trajectories which start in or end at the singular point $r_1 = r_2 = 0$. See also ref. [41.2].

Remark 41.3 Spin and particle exchange symmetry. In our presentation of collinear helium we have completely ignored all dynamical effects due to the spin of the particles involved, such as the electronic spin-orbit coupling. Electrons are fermions and that determines the symmetry properties of the quantum states. The total wave function, including the spin degrees of freedom, must be antisymmetric under the electron-electron exchange transformation. That means that a quantum state symmetric in the position variables must have an antisymmetric spin wave function, i.e., the spins are antiparallel and the total spin is zero (singletstate). Antisymmetric states have symmetric spin wave function with total spin 1 (tripletstates). The threefold degeneracy of spin 1 states is lifted by the spin-orbit coupling.

Remark 41.4 Helium quantum numbers. The classification of the helium states in terms of single electron quantum numbers, sketched in sect. 41.5.1, prevailed until the 1960's; a growing discrepancy between experimental results and theoretical predictions made it necessary to refine this picture. In particular, the different Rydberg series sharing a given N-quantum number correspond, roughly speaking, to a quantization of the inter electronic angle Θ, see figure 41.1, and can not be described in terms of single electron quantum numbers l_1, l_2. The fact that

something is slightly wrong with the single electron picture laid out in sect. 41.5.1 is highlighted when considering the collinear configuration where both electrons are on the *same* side of the nucleus. As both electrons again have angular momentum equal to zero, the corresponding quantum states should also belong to single electron quantum numbers $(l_1, l_2) = (0, 0)$. However, the single electron picture breaks down completely in the limit $\Theta = 0$ where electron-electron interaction becomes the dominant effect. The quantum states corresponding to this classical configuration are distinctively different from those obtained from the collinear dynamics with electrons on different sides of the nucleus. The Rydberg series related to the classical $\Theta = 0$ dynamics are on the outermost rigth side in each N subspectrum in figure 41.6, and contain the energetically highest states for given N, n quantum numbers, see also remark 41.5. A detailed account of the historical development as well as a modern interpretation of the spectrum can be found in ref. [41.1].

Remark 41.5 Beyond the unstable collinear helium subspace. The semiclassical quantization of the chaotic collinear helium subspace is discussed in refs. [41.7, 41.8, 41.9]. Classical and semiclassical considerations beyond what has been discussed in sect. 41.5 follow several other directions, all outside the main of this book.

A classical study of the dynamics of collinear helium where both electrons are on the same side of the nucleus reveals that this configuration is fully stable both in the collinear plane and perpendicular to it. The corresponding quantum states can be obtained with the help of an approximate EBK-quantization which reveals helium resonances with extremely long lifetimes (quasi - bound states in the continuum). These states form the energetically highest Rydberg series for a given principal quantum number N, see figure 41.6. Details can be found in refs. [41.10, 41.11].

In order to obtain the Rydberg series structure of the spectrum, i.e., the succession of states converging to various ionization thresholds, we need to take into account the dynamics of orbits which make large excursions along the r_1 or r_2 axis. In the chaotic collinear subspace these orbits are characterized by symbol sequences of form $(a0^n)$ where a stands for an arbitrary binary symbol sequence and 0^n is a succession of n 0's in a row. A summation of the form $\sum_{n=0}^{\infty} t_{a0^n}$, where t_p are the cycle weights in (41.12), and cycle expansion of indeed yield all Rydberg states up the various ionization thresholds, see ref. [41.4]. For a comprehensive overview on spectra of two-electron atoms and semiclassical treatments ref. [41.1].

Résumé

We have covered a lot of ground starting with considerations of the classical properties of a three-body Coulomb problem, and ending with the semiclassical helium spectrum. We saw that the three-body problem restricted to the dynamics on a collinear appears to be fully chaotic; this implies that traditional semiclassical methods such as *WKB*quantization discussed in chapter 33 will not work and that we needed the full periodic orbit theory to obtain leads to the semiclassical spectrum of helium. As a piece of unexpected

⇓PRIVATE
⇑PRIVATE

luck the symbolic dynamics is simple, and the semiclassical quantization of the collinear dynamics yields an important part of the helium spectrum, including the ground state, to a reasonable accuracy. A sceptic might say: "Why bother with all the semiclassical considerations? A straightforward numerical quantum calculation achieves the same goal with better precision." While this is true, the semiclassical analysis offers new insights into the *structure* of the spectrum. We discovered that the dynamics perpendicular to the collinear plane was stable, giving rise to an additional (approximate) quantum number ℓ. We thus understood the origin of the different Rydberg series depicted in figure 41.6, a fact which is not at all obvious from a numerical solution of the quantum problem.

Having traversed the long road from the classical game of pinball all the way to a credible helium spectrum computation, we could declare victory and fold down this enterprise. Nevertheless, there is still much to think about - what about such quintessentially quantum effects as diffraction, tunnelling, ...? As we shall now see, the periodic orbit theory has still much of interest to offer.

References

[41.1] G. Tanner, J-M. Rost and K. Richter, Rev. Mod. Phys. **72**, 497 (2000).

[41.2] K. Richter, G. Tanner, and D. Wintgen, Phys. Rev. A **48**, 4182 (1993).

[41.3] Bürgers A., Wintgen D. and Rost J. M., J. Phys. B **28**, 3163 (1995).

[41.4] G. Tanner and D. Wintgen Phys. Rev. Lett. **75** 2928 (1995).

[41.5] P. Kustaanheimo and E. Stiefel, *J. Reine Angew. Math.* **218**, 204 (1965).

[41.6] E.L. Steifel and G. Scheifele, *Linear and regular celestial mechanics* (Springer, New York 1971).

[41.7] G.S. Ezra, K. Richter, G. Tanner and D. Wintgen, J. Phys. B **24**, L413 (1991).

[41.8] D. Wintgen, K. Richter and G. Tanner, CHAOS **2**, 19 (1992).

[41.9] R. Blümel and W. P. Reinhardt, *Directions in Chaos Vol 4*, eds. D. H. Feng and J.-M. Yuan (World Scientific, Hongkong), 245 (1992).

[41.10] K. Richter and D. Wintgen, J. Phys. B **24**, L565 (1991).

[41.11] D. Wintgen and K. Richter, Comments At. Mol. Phys. **29**, 261 (1994). why no reference to D. Delande?

[41.12] P. Kustaanheimo, *Ann. Univ. Turku, Ser. AI.,* **73** (1964).

[41.13] T. Levi-Civita, *Opere mathematische* **2** (1956).

[41.14] H. Hopf, *Math. Ann.* **104** (1931).